



# Lawrence Berkeley Laboratory

UNIVERSITY OF CALIFORNIA

## ENERGY & ENVIRONMENT DIVISION

Presented at the SAE International Automotive Engineers  
Congress and Exposition, Detroit, MI, February 25-29, 1980

### PERFORMANCE OF A PLASMA JET IGNITER

B. Cetegen, K. Y. Teichman, F. J. Weinberg,  
and A. K. Oppenheim

January 1980

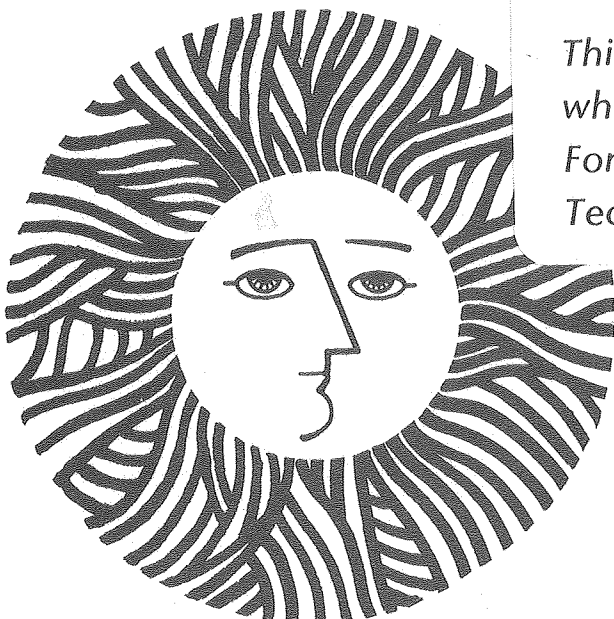
RECEIVED  
LAWRENCE  
BERKELEY LABORATORY

APR 3 1980

LIBRARY AND  
DOCUMENTS SECTION

### TWO-WEEK LOAN COPY

*This is a Library Circulating Copy  
which may be borrowed for two weeks.  
For a personal retention copy, call  
Tech. Info. Division, Ext. 6782.*



LBL 10365 C.2

## **DISCLAIMER**

This document was prepared as an account of work sponsored by the United States Government. While this document is believed to contain correct information, neither the United States Government nor any agency thereof, nor the Regents of the University of California, nor any of their employees, makes any warranty, express or implied, or assumes any legal responsibility for the accuracy, completeness, or usefulness of any information, apparatus, product, or process disclosed, or represents that its use would not infringe privately owned rights. Reference herein to any specific commercial product, process, or service by its trade name, trademark, manufacturer, or otherwise, does not necessarily constitute or imply its endorsement, recommendation, or favoring by the United States Government or any agency thereof, or the Regents of the University of California. The views and opinions of authors expressed herein do not necessarily state or reflect those of the United States Government or any agency thereof or the Regents of the University of California.

Title: PERFORMANCE OF A PLASMA JET IGNITER (1)\*

by : B. Cetegen (2), K. Y. Teichman (3), F. J. Weinberg (4),  
and A. K. Oppenheim (5)

Lawrence Berkeley Laboratory  
University of California  
Berkeley, California 94720

(1)\* This work was supported by NSF Grant ENG78-12372 and  
by the U.S. Department of Energy under Contract No.  
W-7405-ENG-48.

(2) Research Assistant, California Institute of Technology,  
Pasadena.

(3) Assistant Professor, University of Minnesota, Minneapolis.

(4) Professor of Combustion Physics, Imperial College of  
Science and Technology, London, England.

(5) Professor of Mechanical Engineering, University of  
California, Berkeley.



## ABSTRACT

The main advantage of jet igniters lies in their ability to provide distributed ignition sources that are capable of initiating and enhancing combustion in lean mixtures. This is achieved principally by two mechanisms: the provision of a high concentration of free radicals, enhancing ignition at lower temperatures, and of the extended highly turbulent igniting surface, yielding larger flame front areas and hence increased burning rates. The paper describes experimental and analytical procedures that were developed to determine the performance of a jet igniter with particular emphasis on the fluid mechanic effects. This consists of the evaluation of the penetration depth of the jet as a function of the plasma plug geometry, and of the rate of burning in the jet-ignited charge, as well as the corresponding turbulent and laminar flame burning velocities. To de-emphasize the thermochemical effects, the plasma medium and energy were maintained without change for all the tests. Thus the only variables in our study pertained just to the geometry of the igniter, that is, the volume of the cylindrical plasma cavity and the area of the orifice discharging the jet. The results are based on

high speed schlieren cinematography of the combustion process in a cylindrical bomb, and simultaneous pressure transducer measurements. The penetration depth is shown to be proportional to the square root of the characteristic length — the ratio of the volume of igniter cavity to its orifice area. The capability to ignite lean mixtures is demonstrated by the repeatability of results attained with the use of methane-air mixtures at an equivalence ratio of 0.6, initially at atmospheric pressure and room temperature. Under these conditions the observed enhancement of the rate of combustion could be accounted for entirely by the fact that the flame surface was enlarged due to ignition by a highly turbulent jet. While the laminar burning velocity was well within the range reported in the literature, the corresponding 'turbulent' burning velocity was about three times greater, the ratio between the two remaining nearly constant throughout the process.

INITIATION AND MAINTENANCE OF COMBUSTION in lean mixtures requires special means which can be provided by multi-point ignition systems. There are two such systems known at present: torch igniters and jet igniters. The first forms the principal feature of divided-chamber stratified charge engines where the combustion of the lean charge is produced by a highly turbulent flame generated in the precup (1,2,3,4,5). The second produces, as a rule, a turbulent jet rich in radicals that act as high-temperature substitutes for ignition (6,7,8,9). The main difference between the two systems is that the first is associated with a subsonic flow of a burning substance, while the second with a supersonic jet which does not burn, but instead creates a turbulent cloud where the combustion process starts after the elapse of a definite induction time. The usual way of creating such jets is by means of plasma generators, although, as demonstrated by us (10), similar effects can be obtained with the use of combustion generators that, in contrast to torch igniters, maintain a supercritical pressure ratio across the injector orifice.

Torch igniters are better known today and their technology is more advanced. Presented here is a rational approach to the performance evaluation of jet igniters, offered in the hopes that their development will be thereby enhanced.

Jet igniters are associated with the following two advantages:

- 1) As a consequence of their inherent penetration depth, they are capable of initiating combustion in the middle of the charge, away from the walls, thus eliminating all the adverse effects due to their proximity — a significant factor in the enhancement of ignition.
- 2) In contrast to the initially very low burning rate of a typical laminar flame kernel initiated by a conventional spark discharge, they generate a turbulent cloud, where, after a certain induction time, multi-point ignition takes place so that combustion proceeds at a relatively high rate—a consequence of the relatively large surface area of the convoluted flame front thus created.

A fluid mechanical study of these two properties is reported here with respect to the performance of a simple plasma jet igniter, that is, one devoid of any means to modify the plasma

medium or its energy. Thus, unlike our previous investigations (9,10), where special provisions were made for different plasma feed-stock and various amounts of electrical energy supplied to produce the jet, this time, in order to de-emphasize the thermochemical effects, the cavity was filled only through the orifice with the same medium as that initially in the bomb, while for the parametric studies reported here its state and composition were kept invariant, and it was provided with a similar pulse of electrical energy for all the tests. In effect then, the only variables we took into account here pertained to the geometry of the igniter, that is, specifically to the volume of the cylindrical cavity where the plasma was generated and the area of the orifice through which it was discharged.

#### JET PENETRATION

ANALYSIS — The jet is created by efflux from a constant volume reservoir where the medium has

been brought to high pressure and temperature by a rapid deposition of energy.

The energy balance for the process of efflux can be expressed as

$$\frac{d(M_o e_o)}{dt} = h_o \frac{dM_o}{dt} \quad (1.1)$$

where subscript o denotes conditions in the reservoir at any time.\* Since the bulk of mass escapes at critical flow conditions,

$$\frac{dM_o}{dt} = -\left(\frac{2}{\gamma+1}\right)^{\frac{\gamma+1}{2(\gamma-1)}} \frac{a_o}{v_o} A^* \quad (1.2)$$

where  $A^*$  is the effective flow area of the orifice.

Using perfect gas relations,

$$e_o = \frac{a_o^2}{\gamma(\gamma-1)} \quad ; \quad h_o = \frac{a_o^2}{\gamma-1}$$

Equations (1.1) and (1.2) yield

$$\frac{d\alpha}{\alpha} = -\frac{dt}{\tau}$$

where

$$\alpha \equiv \frac{a_o}{a_{oi}} \quad ;$$

$$\tau \equiv \frac{2}{\gamma-1} \left(\frac{\gamma+1}{2}\right)^{\frac{\gamma+1}{2(\gamma-1)}} \frac{L^+}{a_{oi}} \quad ,$$

with subscript i denoting initial conditions while

$$L^+ \equiv \frac{V}{A^*}$$

represents the critical length of the jet generator.†

---

\*Symbols are defined in the Appendix.

†The authors wish to acknowledge their appreciation to Professor A.L.London for bringing their attention to the convenience and appropriateness of this concept.

Integration of Eq. (1.3) gives a hyperbolic law for the decay of the local velocity of sound in the reservoir

$$\alpha = \frac{1}{1 + \frac{t}{\tau}} \quad (1.4)$$

where  $\tau$  plays the role of a time constant, the value of the intersection with the  $t$ -axis of the tangent to the curve at  $t=0$ , delineating the initial slope of the decay.

The jet is considered to be axisymmetric, turbulent, and quasi-steady. Under such circumstances, the mean Lagrangian flow velocity,  $u$ , at any position  $x$ , can be approximated (11) as follows:

$$u = \frac{dx}{dt} = \frac{u_n x_n}{x} \quad (1.5)$$

where subscript  $n$  denotes the section at which the jet can be first considered to become effectively one-dimensional.

Integration of Eq. (1.5), subject to initial conditions  $u=u_n$ ,  $x=x_n$  at  $t=0$ , yields

$$x^2 = x_n^2 + 2u_n x_n t \quad (1.6)$$

Introducing average quantities for the bulk of ejected mass

$$\bar{t} = c_t \quad ; \quad \bar{u}_n = c_u a_{oi}$$

where in the first approximation  $c_t$  and  $c_v$  can be considered to be effectively constant, and noting that  $x_n$  is negligible in comparison to the penetration depth, the latter can be expressed on the basis of Eqs. (1.4) and (1.6) as

$$\bar{x} = \sqrt{KL^+} \quad (1.7)$$

where

$$K = \frac{4}{\gamma-1} \left( \frac{\gamma+1}{2} \right)^{\frac{\gamma+1}{2(\gamma-1)}} c_t c_u x_n \approx \text{const} .$$

In the first approximation of this simple treatment it appears thus that, if the thermochemical conditions of the igniter are invariant, the penetration depth is proportional to the square root of the characteristic length of the plasma generator.

EXPERIMENTS — To check the validity of this simple law, schlieren records were obtained of the jets issuing into air from three simple plasma plugs of different characteristic lengths, namely  $L^+ = 0.765, 1.042$  and  $1.675$  cm. The effective volume of the generator cavity was  $10 \text{ mm}^3$ , and the energy of the electric discharge was  $2.5 \text{ J}$ , the same in all cases, while the working substance as well as the atmosphere into which the jets were ejected was air initially at atmospheric pressure and room temperature.

Schlieren flash photographs of the turbulent clouds formed by the jets, taken  $6 \text{ msec}$  after electric discharge, are displayed in Fig. 1. High-speed cinematographic records demonstrated that the situation recorded there was attained within the first millisecond; after that the cloud was gradually dissipating without an appreciable shift in its position and extent. Jet penetrations evaluated from Fig. 1 are shown, plotted as a function of  $L^+$ , in Fig. 2. As noted there, they can be considered to be fixed either by the outer edge of the cloud or by the center of its outer blob. Lines present the best fit to the data of the relationship specified by Eq. (1.7), confirming the validity of the trend it predicts in both cases.

F.1  
F.2

#### BURNING RATES AND FLAME VELOCITIES

ANALYSIS — The most important feature of the performance of a jet igniter is, of course, the rate of burning and the flame velocity it can induce in a lean mixture. Since combustion starts in a turbulent cloud and the flame front is quite convoluted throughout its life, the process cannot be analyzed in too much detail. On the other hand, flame velocities have to be determined with sufficient precision so that their values could be adequately assessed in comparison to data on laminar flames available in the literature.

The only way to meet these conflicting demands is to consider the reacting system as one consisting essentially of two components, the reactants and the products, while taking carefully into account their properly averaged thermodynamic properties. Since combustion takes place away from the walls and the whole process is of a relatively short duration, the whole system can be considered as essentially adiabatic, while the reactants undergo an isentropic compression due to the expansion of combustion products.

The model of a two-component reacting mixture is well established in the combustion

literature, especially with respect to the analysis of processes occurring in reciprocating piston engines (12). Various analytical approaches to combustion in a constant volume bomb based on this model were critically assessed by Bradley and Mitcheson (13), who demonstrated its validity with reference in particular to the relationship between burned volume and pressure. This, as will be shown later, plays a key role in the method we developed for the interpretation of our data.

For combustion in a two-component system, the conservation of mass in an enclosure whose total volume is  $V_t$ , subject to constraint of a uniform pressure throughout the system, can be expressed as follows:

$$M_u + M_b = M_t = M_i \quad (2.1)$$

$$V_u + V_b = V_t \quad (2.2)$$

$$P_u = P_b = P_t \quad (2.3)$$

where subscripts u, b, t, and i denote respectively unburned, burned, total, and initial values.

Introducing a set of dimensionless variables defined as follows

$$m \equiv \frac{M_b}{M_i} ; \quad n \equiv \frac{V_b}{V_i} ; \quad r \equiv \frac{R_b}{R_i} ;$$

$$x_u \equiv \frac{v_u}{v_i} ; \quad x_b \equiv \frac{v_b}{v_i} ; \quad y \equiv \frac{P_b}{P_i} = \frac{P_u}{P_i} ;$$

$$z_b \equiv \frac{T_b}{T_i} ; \quad z_u \equiv \frac{T_u}{T_i} ; \quad v \equiv \frac{V_t}{V_i} ;$$

and noting that

$$V_k = M_k v_k \quad k = u, b$$

Eqs. (2.1) and (2.2) yield

$$(1-m) + mx_b = v \quad (2.4)$$

Invoking Eq. (2.3), while each component is assumed to behave as a perfect gas, so that

$$rz_b = x_b y ; \quad z_u = x_u y ,$$

one thus obtains

$$rz_b m = vy - (1-m)z_u \quad (2.6)$$

Taking into account the energy balance for the burned gas, which in the context of our model requires the heat of combustion to be uniformly distributed as internal energy of the products, it follows that

$$d(z_b m) = z_f dm \quad (2.7)$$

where subscript  $f$  denotes the adiabatic flame temperature.

Differentiating Eq. (2.6) and combining with Eq. (2.7) one thus obtains the following relation between the burned mass and pressure

$$\frac{dm}{dy} = \frac{v - (1-m)(dz_u/dy)}{rz_f - z_u} \quad (2.8)$$

Flame temperatures for a methane-air mixture at an equivalence ratio  $\phi = 0.6$  and initial atmospheric pressure and room temperature were computed by the use of the NASA CEC Program (14). The results are presented in Fig. 3. Shown there also are the temperatures of compressed reactants corresponding to the same initial conditions, evaluated for the same mixture taking into account the variation of specific heats with temperature according to JANAF Tables (15).

Plots of Fig. 3 can be expressed with sufficient accuracy by the relations

$$z_f = z_{fi} y^\alpha \quad ; \quad z_u = y^\beta \quad (2.9)$$

where the indices  $\alpha$  and  $\beta$  are essentially constant. Hence Eq. (2.8) becomes

$$\frac{dm}{dy} = \frac{v - \beta(1-m)y^{\beta-1}}{rz_{fi}y^\alpha - y^\beta} \quad (2.10)$$

Values of  $\alpha$ ,  $z_{fi}$  and  $\beta$  computed by the use of the CEC Code (14) for methane-air mixtures over a range of equivalence ratios,  $0.4 \leq \phi \leq 1.0$ , are listed in Table 1. To provide a sense of value, included there also are the magnitudes of the equivalent specific heat ratios of perfect gases with constant specific heats that would display the same variation of temperature with pressure in an isentropic process,

$$\gamma_\alpha = (1-\alpha)^{-1} \quad \text{and} \quad \gamma_\beta = (1-\beta)^{-1}.$$

Equation (2.10) has been integrated by the Runge-Kutta technique for the initial condition:

Table 1. - Constants in Eq. (2.9) and the  
equivalent specific heat ratios.

$\phi$	$\alpha$	$\gamma_{\alpha}$	$z_{fi}$	$\beta$	$\gamma_{\beta}$
0.40	0.070	1.075	4.01	0.2795	1.388
0.50	0.063	1.067	4.60	0.2795	1.388
0.53	0.061	1.065	4.80	0.2789	1.387
0.54	0.058	1.062	4.87	0.2787	1.386
0.60	0.051	1.054	5.22	0.2767	1.383
1.00	0.035	1.036	7.10	0.2761	1.381

$m(y) = 0$  at  $y=1$ , so that initially

$$\left(\frac{dm}{dy}\right)_{y=1} = \frac{v - \beta}{rz_{fi} - 1} \quad (2.11)$$

In our case, as indicated by the results of equilibrium computations,  $r=1$ , while, as appropriate for a constant volume bomb,  $v=1$ . Equations (2.10) and (2.11) provide an interesting commentary on the simple law, due to Lewis and von Elbe (16) and used by Bradley and Mitcheson (13) in their simplified analyses, of linear dependence of burned mass on pressure. Evidently, in order for this law to hold true, the variation of temperature with pressure must be negligibly small so that  $\alpha = \beta = 0$ . Under such circumstances the law is expressed de facto by Eq. (2.11).

Since by virtue of Eq. (2.4)

$$n = mx_b = v - (1-m)x_u \quad (2.12)$$

Eq. (2.10) also provides information required to evaluate the relationship between the burned volume and pressure.

The results, computed for methane-air mixtures corresponding to equivalence ratios  $\phi = 0.5, 0.6$  and  $1$ , are shown in Fig. 4.

Now the flame burning velocity

$$S_u = \frac{v_u}{A_f} \frac{dM_b}{dt} \quad (2.13)$$

can be expressed on the basis of Eq. (2.10) in terms of the following non-dimensional parameter.

$$\frac{S_u A_f}{v_t (dy/dt)} = x_u \frac{dm}{dy} = y^{\beta-1} \frac{v - \beta(1-m)y^{\beta-1}}{rz_{fi} y^{\alpha} - y^{\beta}} \quad (2.14)$$

which, it should be observed, is a function of the pressure ratio,  $y$ , only. Plots of this parameter for methane-air mixtures corresponding to equivalence ratios  $\phi = 0.5, 0.6$  and  $1.0$ , for which  $r=1$  while  $v=1$ , are presented in Fig. 5.

EXPERIMENTS — Experimental tests of the igniters were performed in a cylindrical, stainless steel bomb, fitted with optical glass windows of schlieren quality, providing an unobstructed view of the cylindrical cavity. The total volume of the bomb was  $530.6 \text{ cm}^3$ , while the port diameter was  $8.58 \text{ cm}$ . On the sides, the bomb was equipped with four instrument plugs. One provided a fitting for the igniter. Two were used for

filling and purging, and the fourth served as holder for a Kistler 601A pressure transducer. Its signal, processed through a charge amplifier, was displayed on the screen of a Tektronix 549 storage oscilloscope. Concurrently with pressure records, high-speed schlieren movies were obtained using a Redlake Hycam camera operating at a speed of 5500 frames per second. The experiments were monitored electronically so that when the camera was brought up to speed it provided a signal for triggering the discharge in the plasma cavity. At the same time the oscilloscope sweep was triggered and a time mark flashed upon the edge of the film. Schlieren cinematography was thus synchronized with pressure measurement.

The same plasma plugs were of course used as those employed to produce the records shown in Fig. 1. Their characteristic lengths were 0.765, 1.042 and 1.675, while the volume of the discharge chamber was  $10 \text{ mm}^3$ . The energy of electric discharge fed to the cavity was 2.5J. Experimental results obtained with these plugs igniting a methane-air mixture at an equivalence ratio of 0.6, initially at atmospheric pressure and room temperature, are presented in Figs. 6, 7 and 8, respectively. Each set consists of the pressure transducer record and four schlieren photographs reproduced from cinematographic frames at 1, 10, 20 and 30 msec after the electric discharge. In all cases the flame reaches the side walls at about 30 msec so that all the significant results were provided only by the first part of the pressure record. We have found that this can be expressed with good precision in terms of the relation

$$y = e^{\delta(t-\theta)} \quad (2.15)$$

where  $t$  is in milliseconds, while  $\delta$  and  $\theta$  are given in Table 2.

It had been our intention to perform the tests as closely as possible to the lean ignition limit. For the methane-air mixture at STP, such a limit corresponds to 5.3 volumetric fraction of methane (17). However, in the immediate vicinity of this limit our results displayed an excessive dependence on mixture composition, as manifested, for example, by significant variation in pressure response to small changes in composition which were beyond our control. At an equivalence ratio of 0.6, on the other hand, the reproducibility of our results was most satisfactory and for this reason we adopted this composition for all the tests.

Table 2 - Constants in Eq. (2.15).

$L^+$ (cm)	$\delta$ (msec <sup>-1</sup> )	$\theta$ (msec)
0.765	0.01252	4.0
1.042	0.01045	4.0
1.675	0.01489	3.0

INTERPRETATION — The derivation of reliable information on flame velocity depends crucially on proper interpretation of the two-dimensional schlieren image of the expanding volume of burned gases. In this respect one is aided by the intrinsic property of the schlieren image in that it provides a record of those portions of the flame front which are parallel to the optical axis. Consequently, schlieren cinematography provides directly all the information concerning the motion of the outer contour of the burned gas in the direction perpendicular to the optical axis (18). However, we have no means to observe the expansion of the surface of the burned gas in other directions. Information about this can be deduced, nonetheless, from the pressure record in the following manner.

As indicated by Eq. (2.14) and displayed by Fig. 5, the flame burning velocity can be evaluated from pressure records, provided that the relationship between the flame surface,  $A_f$ , and pressure ratio  $y$  is known. On the other hand, the relationship between the burned volume, bounded by this surface, and pressure is fixed by Eq. (2.11), as shown by Fig. 4. The method we developed is thus based on an approximate extrapolation to three-dimensional space of the two-dimensional image of the flame front and then its proper adjustment to satisfy Eq. (2.11).

The extrapolation is based upon the postulate that, on the average, the expansion of the burned medium is the same in all directions. Its volume at any instant is therefore estimated from the schlieren image by considering it as the orthogonal projection of a body of revolution. The estimate is aided by the fact that throughout the most significant period of its growth the schlieren image can be approximated by a circle so that the body of burned medium can be treated then as if it were practically spherical. At the same time, the burned volume is evaluated on the basis of Eq. (2.11) by the use of the pressure record expressed in terms of Eq. (2.15).

INTERPRETATION — The derivation of reliable information on flame speeds depends crucially on proper interpretation of the two-dimensional schlieren image of the expanding volume of burned gases. In this respect one is aided by the intrinsic property of the schlieren image in that it provides a record of those portions of the flame front which are parallel to the optical axis. Consequently, schlieren cinematography provides direct information on the motion of the outer contour of the burned gas (18). However, we have no means to observe the expansion of the surface of the burned gas in other directions. Information about this can be deduced, nonetheless, from the pressure record in the following manner.

As indicated by Eq. (2.14) and displayed by Fig. 5, the flame burning speed can be evaluated from pressure records, provided that the relationship between the flame surface,  $A_f$ , and pressure ratio  $\gamma$  is known. On the other hand, the relationship between the burned volume, bounded by this surface, and pressure is fixed by Eq. (2.11), as shown by Fig. 4. The method we developed is thus based on an approximate extrapolation to three-dimensional space of the two-dimensional image of the flame front and then its proper adjustment to satisfy Eq. (2.11).

The extrapolation is based on the only available hypothesis, namely that the burned volume is sufficiently well approximated by that of a body of revolution generated by rotation around the vertical axis of symmetry of the two-dimensional projection of the flame surface recorded by the schlieren image. At the same time, the burned volume is evaluated on the basis of Eq. (2.11) by the use of the pressure record expressed in terms of Eq. (2.15).

The results for the three plasma plugs we tested are presented in Figs. 9, 10 and 11. The continuous lines were obtained from pressure records, while the circles denote values deduced from the cinematographic schlieren photographs. It turned out that the continuous lines are straight — a circumstance that greatly simplified the adjustment between the two sets of records. In order to attain a satisfactory fit, one thus had to introduce only two parameters: a pressure time lag and a fictitious total volume of the reacting gas. Their respective values are noted on the graphs.

The time lag is apparently due to the delay between the discharge in the plasma plug cavity and the moment when the amount of burned gas became sufficiently large to cause a definite response of the pressure transducer. The period

F.9,10  
11

of 3 to 4 milliseconds we noted is certainly quite reasonable under our operating conditions.

The reason why a fictitious volume had to be used is interpreted as a consequence of the intrinsic asymmetry of the flame surface. The burned volume deduced from the two-dimensional schlieren image differs from its actual value evidently because of dissimilarities in other directions than the normal to optical axis that was recorded photographically. The ratio of the fictitious volume,  $V_t'$ , to the actual total volume of the gas,  $V_t$ , specifies then the correction factor for the flame surface area

$$\eta \equiv \frac{A_f}{A_f'} = \left( \frac{V_t}{V_t'} \right)^{2/3} \quad (2.16)$$

where  $A_f$  is the actual area while  $A_f'$  is that deduced from the schlieren image. Values of this factor are also noted on the graphs. Again they appear to be quite reasonable, with a possible exception of that in Fig. 9.

With the proper relationship between the burned volume and pressure thus established, the evaluation of flame burning velocities can be accomplished by combining the information on the growth of the burned volume derived from the pressure record with that on the variation of the flame surface deduced from schlieren photographs.

On the basis of Eq. (2.14) one can determine the product  $S_u A_f$  with the use of the recorded  $y(t)$ , taking into account only the time lag. The results corresponding to Figs. 6, 7 and 8 are shown in Fig. 12.

The only remaining task in the determination of  $S_u$  then is the evaluation of  $A_f$ . Here there are two possibilities: one can consider  $A_f$  either as the smallest surface embodying the burned volume or as the surface of the combustion front taking into account all its wrinkles. The first corresponds, in effect, to the 'turbulent' flame velocity, while the second to its laminar counterpart.

For the first we determined the area of the combustion zone,  $A_p$ , as recorded by the schlieren image, by measuring the area of the image with a planimeter. The turbulent flame front area was then taken to be that of the surface of a sphere whose great circle area is equal to  $A_p$ . For the second we determined the circumference of the combustion zone,  $\ell$ , as recorded on the schlieren image, by evaluating the length of its contour with the use of a map distance

measuring gauge. The laminar flame front area was then taken to be that of the surface of a sphere, the circumference of whose great circle is equal to  $\ell$ . Taking into account the correction factor of (2.16), the turbulent flame front area is given by

$$A_{ft} = 4\eta A_p \quad (2.17)$$

while the laminar flame front area is determined by

$$A_{\ell t} = \frac{2}{\pi} \ell^2 \quad (2.18)$$

The 'turbulent' burning velocities evaluated in this manner are displayed in Fig. 13 and the corresponding laminar velocities are presented in Fig. 14.

In order to provide proper basis for comparison between these results and those available in the literature, the laminar flame speeds have to be corrected so that the effects of elevated pressures and temperatures immediately ahead of the flame are eliminated. The temperature dependence of flame speeds can be expressed, according to Andrews and Bradley (19), as follows:

$$\frac{S_u^{T_0} - 10}{S_u^T - 10} = \left( \frac{T_0}{T} \right)^2 \quad (2.19)$$

where  $S_u$  is in cm/sec. The relationship expressed above has been shown to be valid over a temperature range  $298^\circ\text{K} \leq T \leq 1000^\circ\text{K}$ . The pressure dependence of laminar burning velocities was correlated by Gaydon and Wolfhard (20) in the form

$$\frac{S_u^{P_0}}{S_u^P} = \left( \frac{P_0}{P} \right)^n \quad (2.20)$$

with typical values for  $n$  specified as a function of flame burning velocity at standard temperature. For this reason pressure correction can be made only after the temperature correction has been taken into account.

Laminar burning velocities corrected by the use of Eqs. (2.19) and (2.20) to those corresponding to standard temperature and pressure of the reactants are shown in Fig. 15. According to the data correlated from the literature by Andrews and Bradley (19), laminar burning velocities for methane-air mixtures at an

equivalence ratio of 0.6 are in the range of 6 to 17 cm/sec. The asymptotic values of the curves presented in Fig. 15 fall well within this range.

One can thus conclude that the flame fronts we observed decayed to the appropriate levels of laminar burning velocities in the combustible medium used for our tests. The recorded relatively high rates of combustion are due entirely to the fact that the flame front was convoluted throughout its existence.

It is important to realize that, although these convoluted flame fronts have here been treated as if they were turbulent flames, they do not propagate into a turbulent medium and therefore do not have a fine structure characteristic of turbulent combustion. Thus the high intensity of turbulence in engines and consequent increases in transport properties would produce effects additional to those recorded here. It is clear from the schlieren pictures that in our flames the convolutions become progressively larger and smoother due to what is fundamentally laminar propagation of an initially highly corrugated front.

In order to convey the extent to which the velocity was affected in this manner, ratios of turbulent to laminar velocities are displayed in Fig. 16. As is apparent there, the effect of the convolutions of the flame front is sustained throughout the whole process of combustion in the bomb at a uniform level corresponding to a three-fold augmentation of the effective burning velocity. This implies that the smoothing and enlarging of the convolutions keeps the factor by which the flame area is increased approximately constant. The important conclusion which emerges from this is that whereas chemical effects due to active radicals in the plasma may die out quickly, the fluid mechanical effects persist over an appreciable amount of time.

#### REFERENCES

- (1) M.C.Turkish, "3-Valve Stratified Charge

0.6 are in the range of 6 to 17 cm/sec. The asymptotic values of the curves presented in Fig. 15 fall well within this range.

One can thus conclude that the flame fronts we observed decayed to the appropriate levels of laminar flame speeds in the combustible medium used for our tests. The recorded relatively high rates of combustion are due entirely to the fact that the flame front was turbulent throughout its existence.

In order to convey the extent to which the flame speed was affected in this manner, ratios of turbulent to laminar speeds are displayed in Fig. 16. As it appears there, the effect of turbulence is sustained throughout the whole process of combustion in the bomb at a uniform level corresponding to a three-fold augmentation of the flame speed.

#### REFERENCES

- (1) M.C.Turkish, "3-Valve Stratified Charge Engines: Evolvment, Analysis and Progression," paper 741163 presented at the SAE International Stratified Charge Engine Conference, Michigan, October-November 1974.
- (2) L.A.Gussak, "High Chemical Activity of Incomplete Combustion Products and a Method of Prechamber Torch Ignition for Avalanche Activation of Combustion in Internal Combustion Engines," paper 750890 presented at SAE Automobile Engineering Meeting, Michigan, October 1975.
- (3) L.A.Gussak and M.C.Turkish, "Lag-Process of Combustion and Its Application in Automobile Gasoline Engines," Stratified Charge Engines I, Mech. E., 137-145, London, 1976.
- (4) F.A.Wyczalek, J.L.Harned, S.Maksymiuk, and J.R.Blevins, "EFI Prechamber Torch Ignition of Lean Mixtures," paper 750351 presented at SAE Automotive Engineering Congress and Exposition, Michigan, 1975.
- (5) L.A.Gussak, V.P.Karpov, and Yu.V.Tikhonov, "The Application of Lag-Process in Prechamber Engines," paper 790692 presented at SAE Passenger Car Meeting, Michigan, 1979.
- (6) D.R.Topham, P.R.Smy, and R.M.Clements, "An Investigation of a Coaxial Spark Igniter with Emphasis on its Practical Use," Combustion and Flame 25, 187-195, 1975.
- (7) J.R.Asik, P.Piatkowski, M.J.Foucher, and W.G.Rado, "Design of a Plasma Jet Ignition System for Automotive Applications," paper 770355 presented at SAE Annual Meeting, Michigan, 1977.

- (8) D.J.Fitzgerald, "Pulsed Plasma Igniter for Internal Combustion Engines," paper 760764 presented at SAE Automobile Engineering Meeting, Michigan, 1976.
- (9) F.J.Weinberg, K.Hom, A.K.Oppenheim, and K.Teichman, "Ignition by Plasma Jet," *Nature* 272, 5651, 341-343, March 23, 1978.
- (10) A.K.Oppenheim, K.Teichman, K.Hom, and H.E. Stewart, "Jet Ignition of an Ultra-Lean Mixture," paper 780637 presented at SAE Passenger Car Meeting, Michigan, 1978.
- (11) G.N.Abramovich, "The Theory of Turbulent Jets," Cambridge, MA: The MIT Press, 1963.
- (12) R.B.Krieger and G.L.Borman, "The Computation of Apparent Heat Release for Internal Combustion Engines," paper 66-WA/DGP-4 presented at ASME Annual Meeting and Energy Systems Exposition, New York, November-December 1966.
- (13) D.Bradley and A.Mitcheson, "Mathematical Solutions for Explosions in Spherical Vessels," *Combustion and Flame* 26, 201-217, 1976.
- (14) S.Gordon and B.J.McBride, "Computer Program for Calculations of Complex Chemical Equilibrium Compositions, Rocket Performance, Incident and Reflected Shocks and Chapman-Jouguet Detonations," NASA Report SP-273, 1971.
- (15) Office of Standard Reference Data, "JANAF Thermochemical Tables," National Bureau of Standards Report NSRDS-NBS 37, 1971.
- (16) B.Lewis and G.von Elbe, "Determination of the Speed of Flames and the Temperature Distribution in a Spherical Bomb from Pressure-Time Explosion Records," *Journal of Chemical Physics* 2, 283-290, 1934.
- (17) H.F.Coward and G.W.Jones, "Limits of Flammability of Gases and Vapors," Bulletin 503, Bureau of Mines, U.S.Government Printing Office, Washington, D.C., 1952.
- (18) F.J.Weinberg, "Optics of Flames," London: Butterworths, x+251 pp., 1963.
- (19) G.E.Andrews and D.Bradley, "The Burning Velocity of Methane-Air Mixtures," *Combustion and Flame* 19, 275, 1972.
- (20) A.G.Gaydon and H.G.Wolfhard, "Flames—Their Structure Radiation and Temperature," 4th edition, London: Chapman & Hall, xiii+449 pp., 1979.

## APPENDIX — Nomenclature

### Symbols:

a	speed of sound
A	area
A*	effective flow area
D	diameter
e	specific internal energy
h	specific enthalpy
ℓ	length of contour
L <sup>+</sup>	characteristic length
m	mass fraction
M	mass
n	volume fraction
P	pressure
r	gas constant ratio
R	perfect gas constant
t	time
T	temperature
u	flow velocity
v	specific volume
V	volume
x	distance
y	pressure ratio
z	temperature ratio
α	sound speed ratio or exponent defined in Eq. (2.9)
β	exponent defined in Eq. (2.9)
γ	specific heat ratio
δ	constant defined in Eq. (2.15)
η	correction factor for the flame front area
θ	constant defined in Eq. (2.15)
ν	ratio of the instantaneous chamber volume to its initial value
τ	time constant in Eq. (1.3)
φ	equivalence ratio

### Subscripts:

b	denotes state of burned gas
f	denotes flame property
i	denotes initial value
ℓ	denotes laminar
o	denotes reservoir conditions
p	denotes value determined by planimetry
t	denotes total value or turbulence
u	denotes state of unburned gas or relative to unburned gas

#### FIGURE CAPTIONS:

Fig. 1 - Jet penetration depths at 6 msec after electric discharge in plasma plug cavity. (a)  $L^+ = 0.765$  cm; (b)  $L^+ = 1.042$  cm; (c)  $L^+ = 1.675$  cm.

Fig. 2 - Dependence of the jet penetration depth on the characteristic length.

Fig. 3 - Temperature ratios for isentropic compression and the corresponding adiabatic flame in a methane/air mixture at an equivalence ratio  $\phi = 0.6$ .

Fig. 4 - Relationship between the burned volume fraction and the pressure ratio for methane/air mixtures at equivalence ratios  $\phi = 0.5, 0.6$  and  $1.0$ .

Fig. 5 - Non-dimensional flame speed parameter as a function of pressure ratio for methane/air mixtures at equivalence ratios  $\phi = 0.5, 0.6$  and  $1.0$ .

Fig. 6 - Schlieren photographs and pressure record of combustion process in a methane/air mixture at  $\phi = 0.6$  ignited by plasma jet igniter with  $L^+ = 0.765$  cm. Schlieren photographs: (a) 1 msec; (b) 10 msec; (c) 20 msec; (d) 30 msec. Pressure record: pressure, 10 psi/div; time, 20 msec/div.

Fig. 7 - Schlieren photographs and pressure record for the combustion process in a methane/air mixture at  $\phi = 0.6$ , ignited by plasma jet igniter with  $L^+ = 1.042$  cm. Schlieren photographs: (a) 1 msec; (b) 10 msec; (c) 20 msec; (d) 30 msec. Pressure record: pressure, 10 psi/div; time, 20 msec/div.

Fig. 8 - Schlieren photography and pressure record of combustion process in a methane/air mixture at  $\phi = 0.6$  ignited by plasma jet igniter with  $L^+ = 1.675$  cm. Schlieren photographs: (a) 1 msec; (b) 10 msec; (c) 20 msec; (d) 30 msec. Pressure record: pressure, 10 psi/div; time, 20 msec/div.

Fig. 9 - Correlation between the variation of burned volume deduced from schlieren cinematography and that determined from the pressure record for tests using plasma jet igniter with  $L^+ = 0.765$  cm.

Fig. 10 - Correlation between the variation of burned volume deduced from schlieren cinematography and that determined from the pressure records for tests using plasma jet igniter with  $L^+ = 1.042$  cm.

Fig. 11 - Correlation between the variation of burned volume deduced from schlieren cinematography and that determined from the pressure record for tests using plasma jet igniters with  $L^+ = 1.675$  cm.

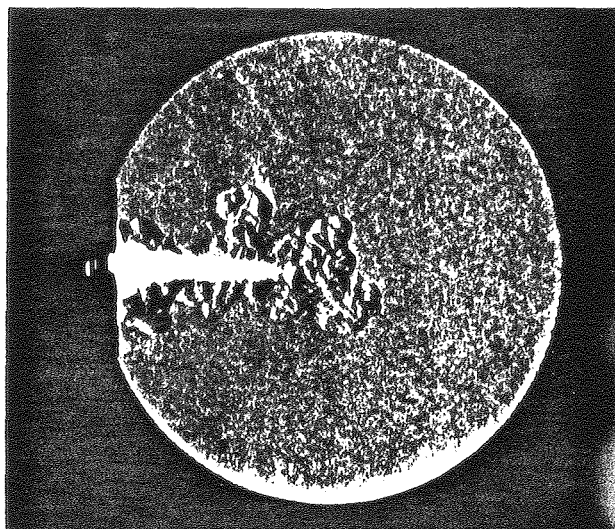
Fig. 12 - Product of the burning velocity and its frontal area deduced from pressure records.

Fig. 13 - Turbulent burning velocities.

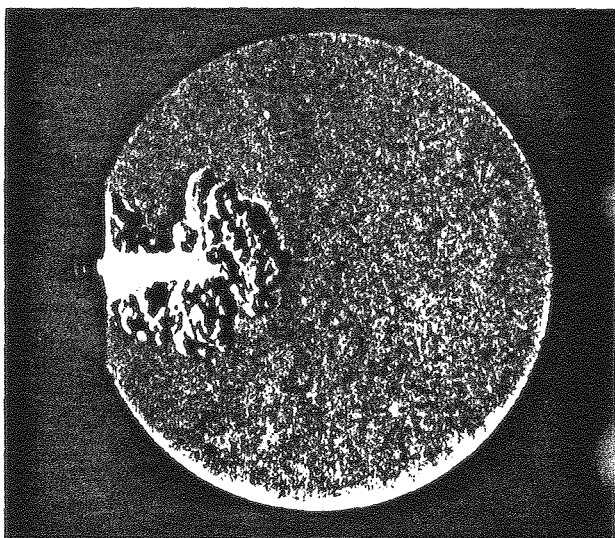
Fig. 14 - Laminar burning velocities.

Fig. 15 - Laminar burning velocities corresponding to STP conditions of reactants.

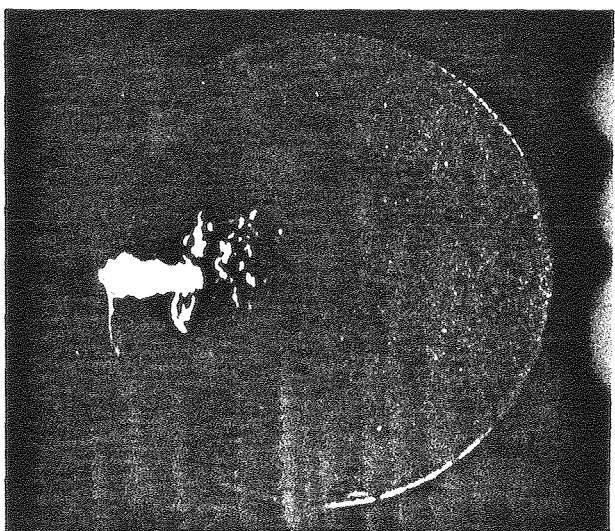
Fig. 16 - Ratio of turbulent to laminar burning velocities.



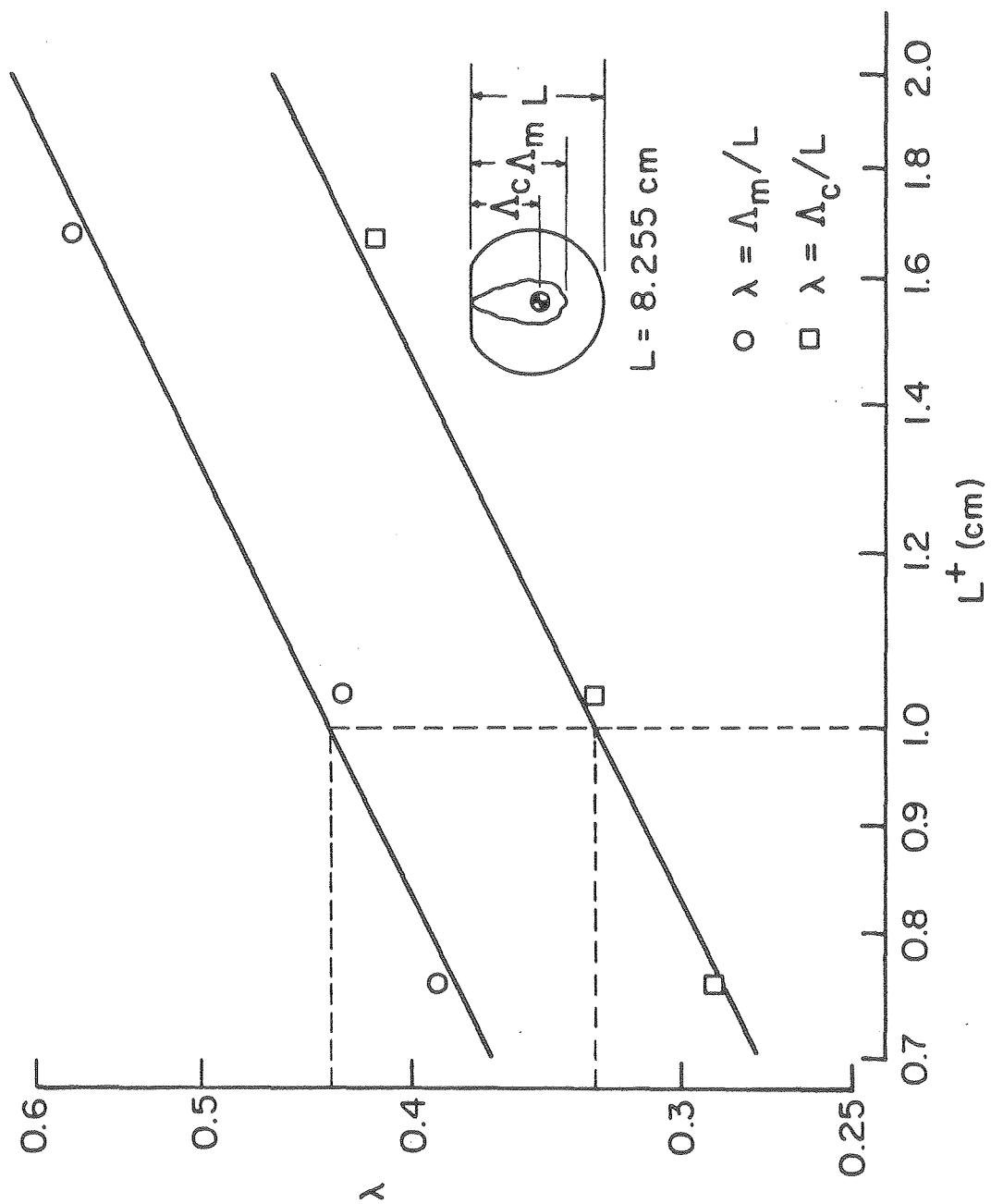
c



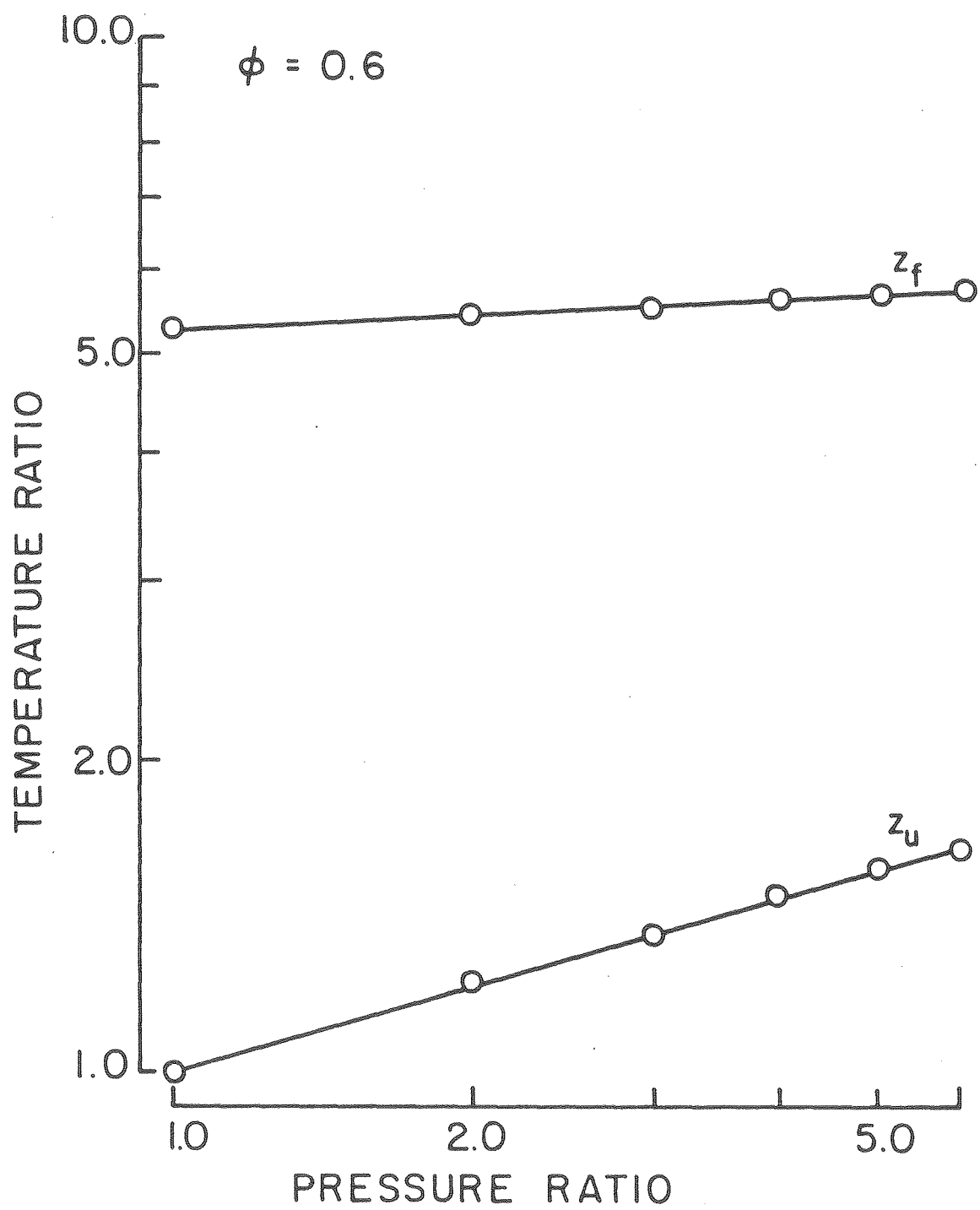
b



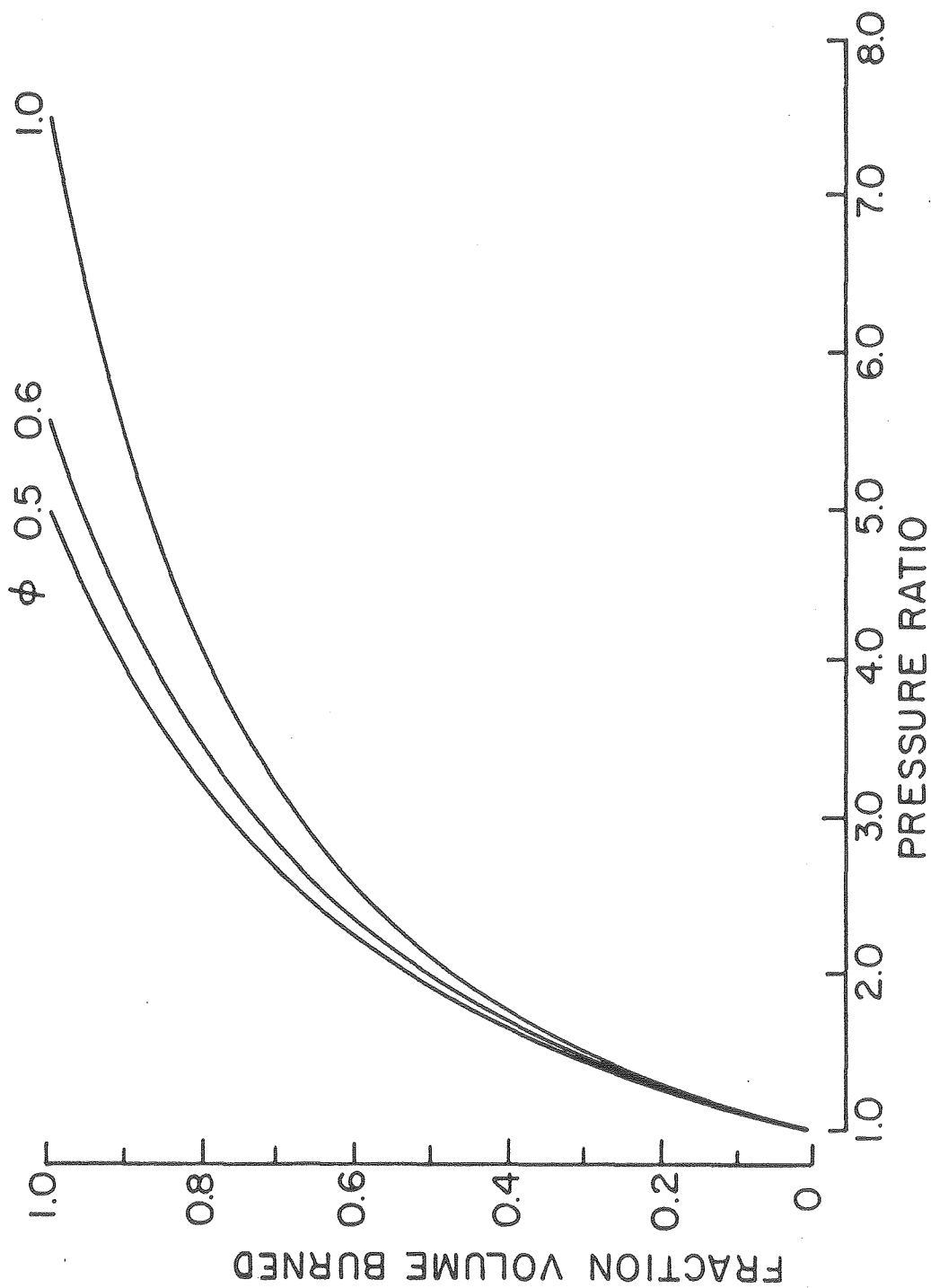
a



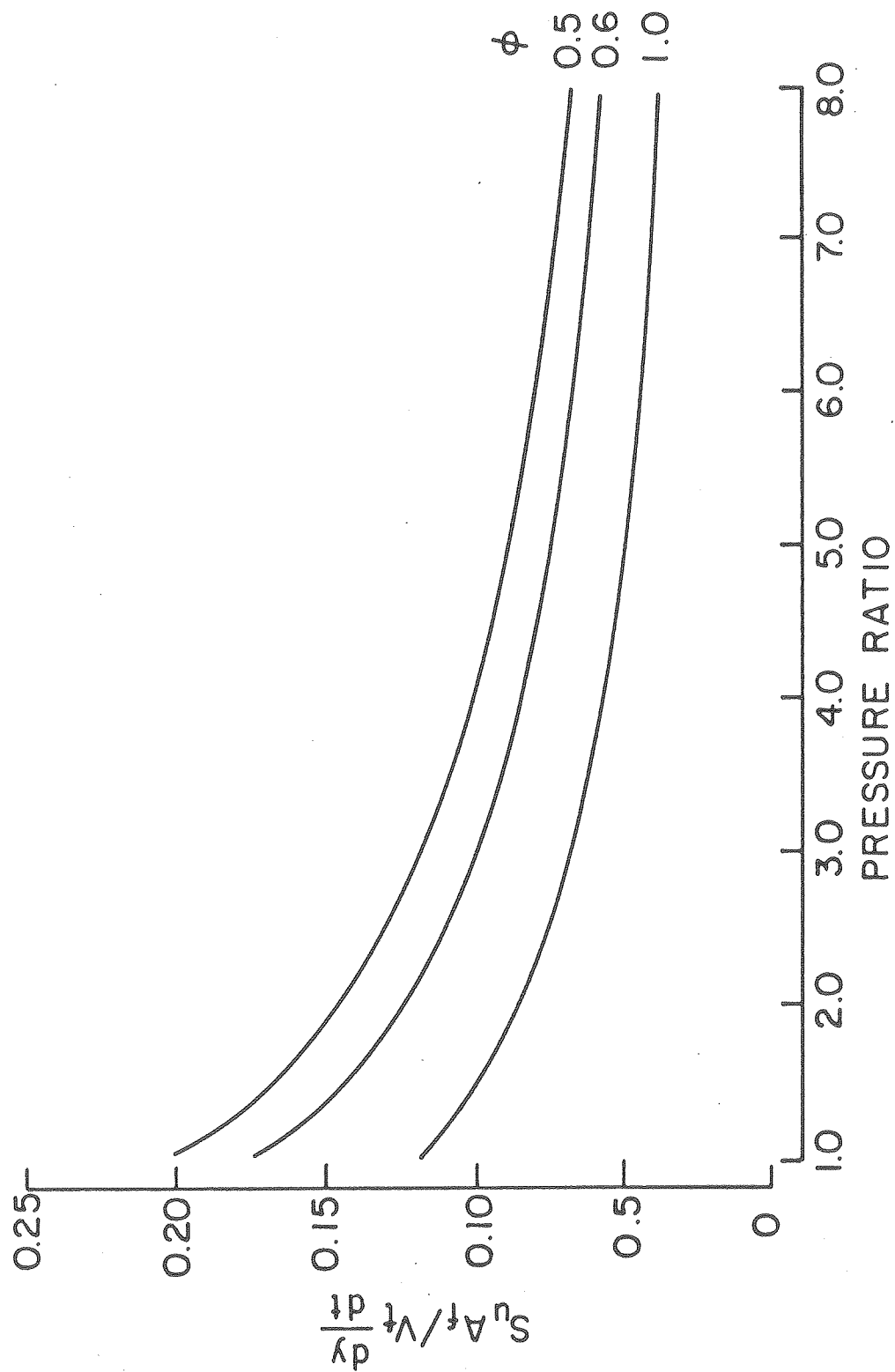
XBL 798 - 6785



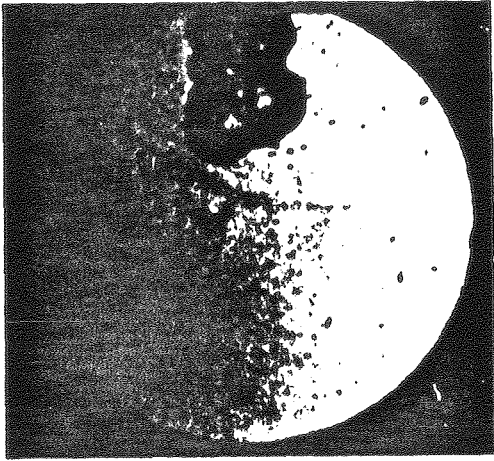
XBL798-6772



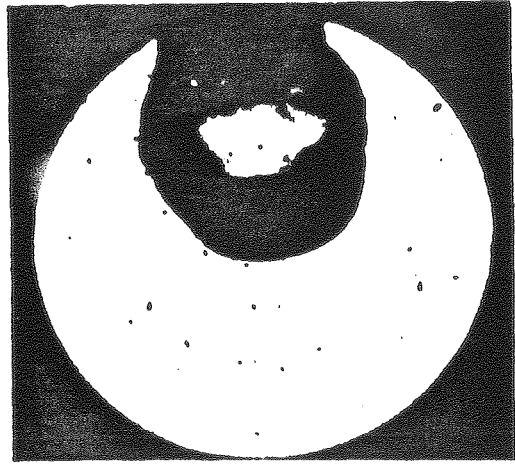
XBL 798-6775



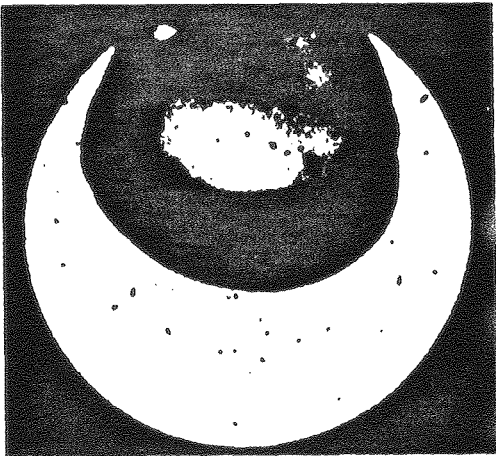
XBL798-6776



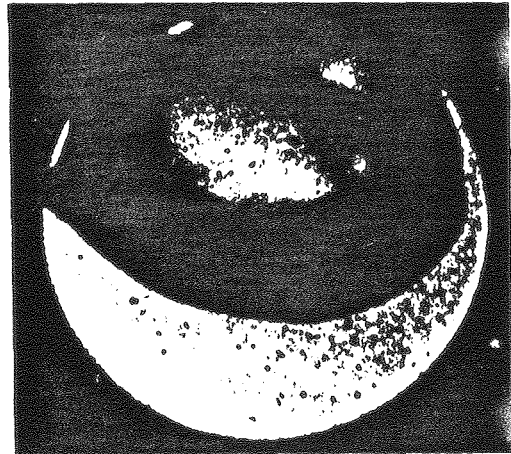
a



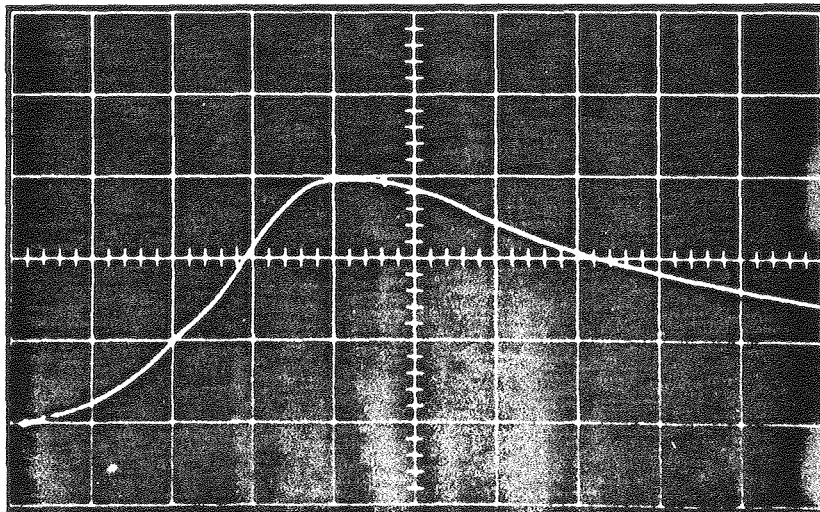
b

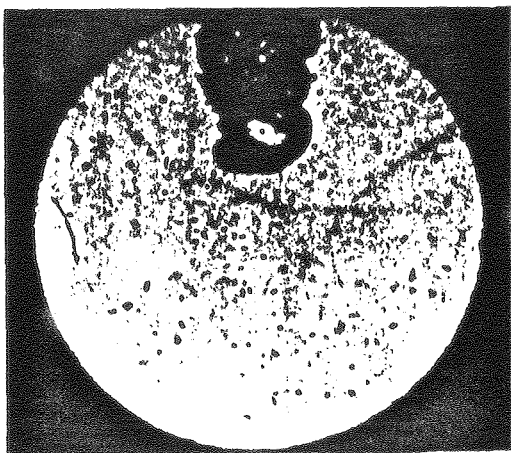


c



d

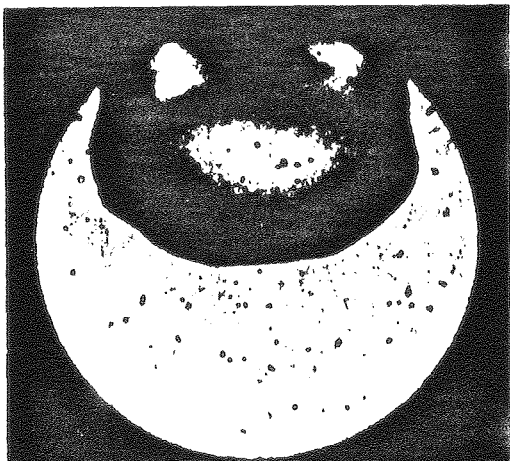




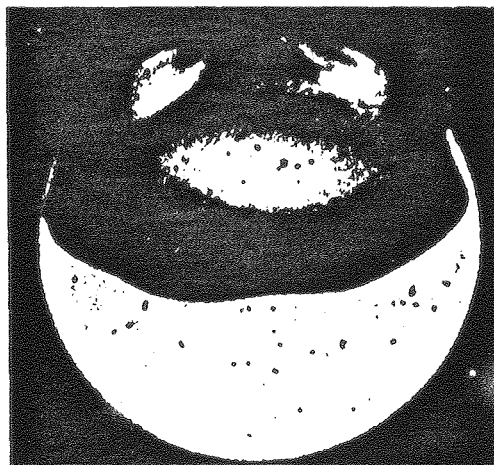
a



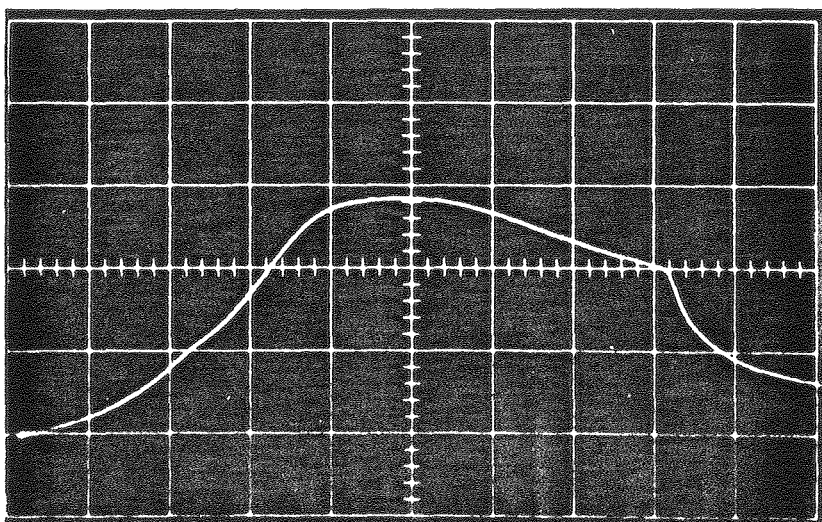
b

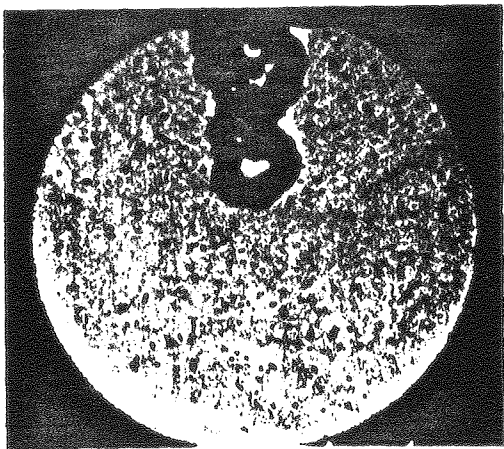


c

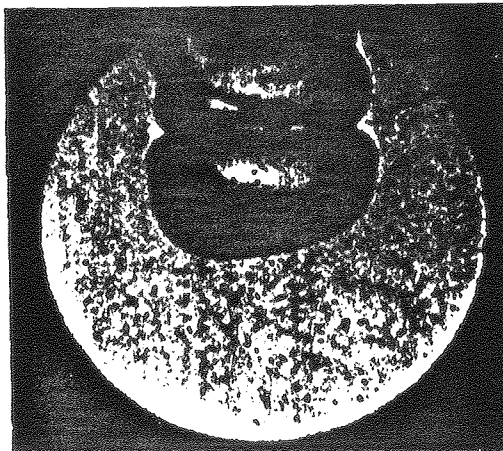


d

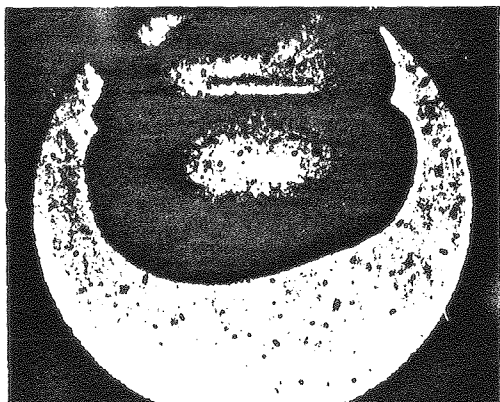




a



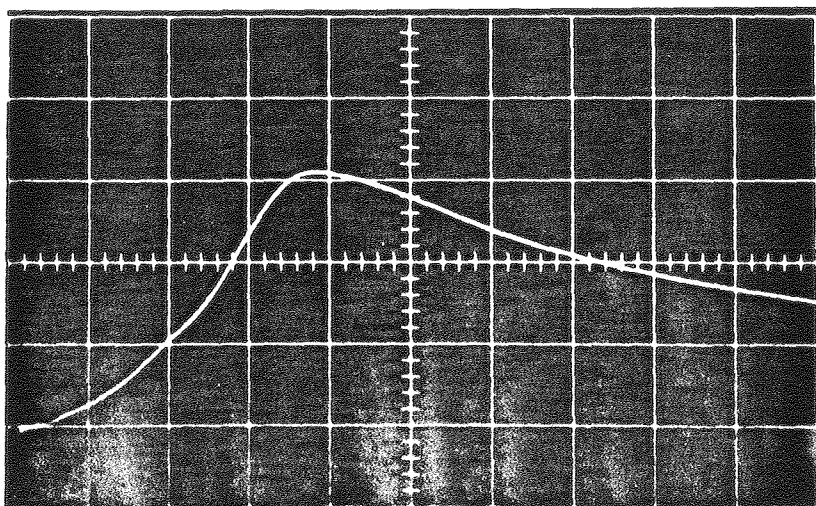
b

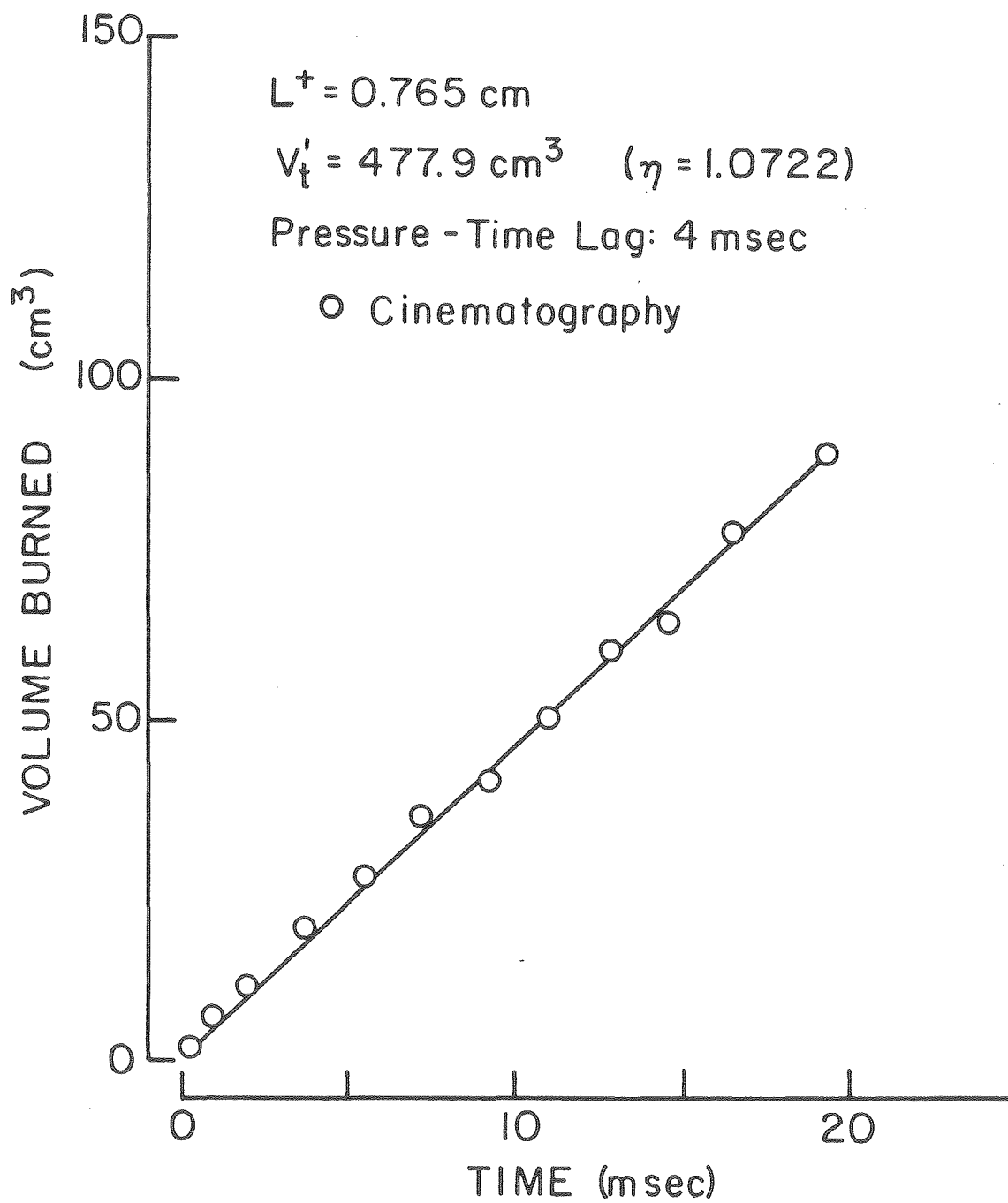


c

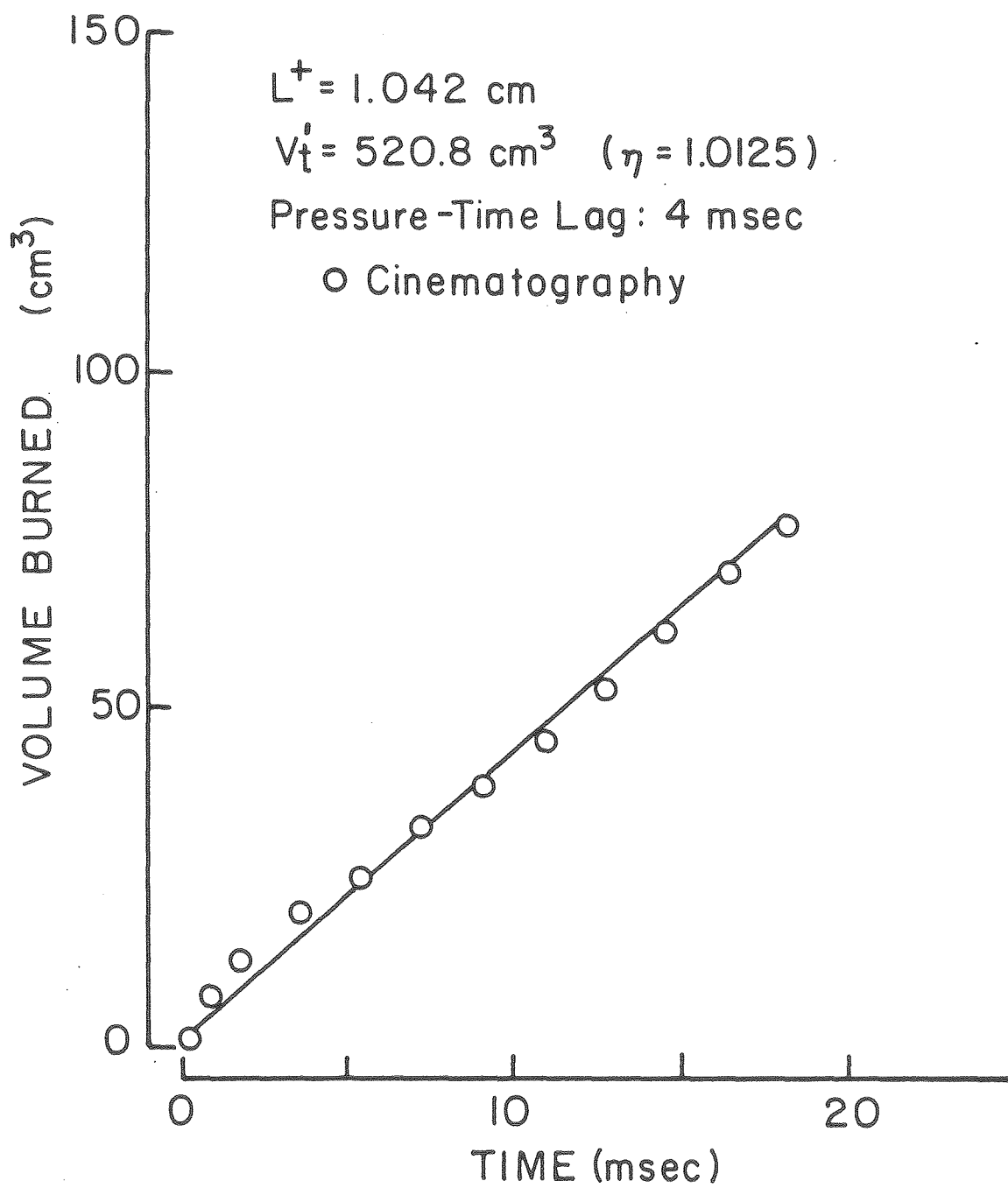


d

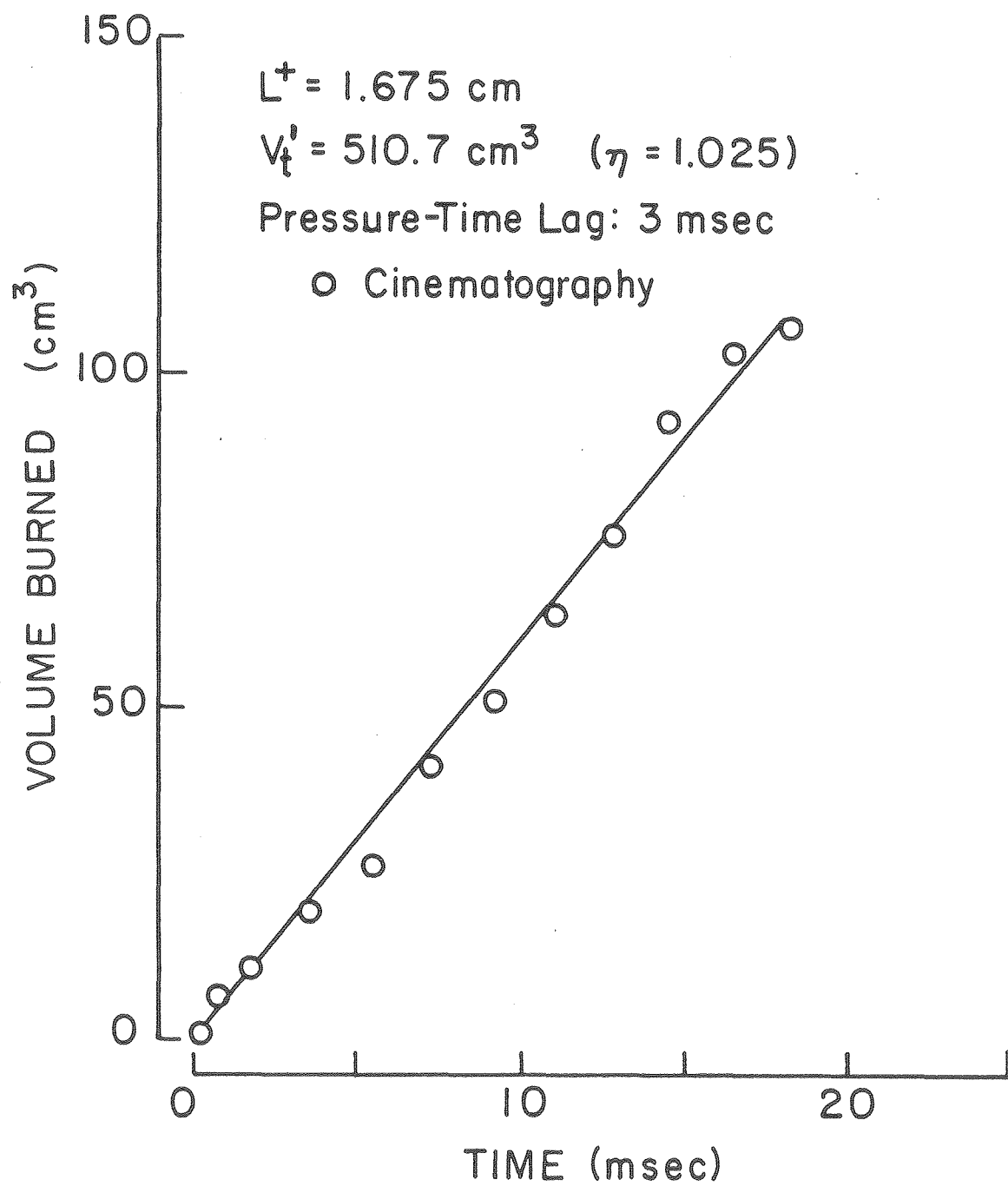




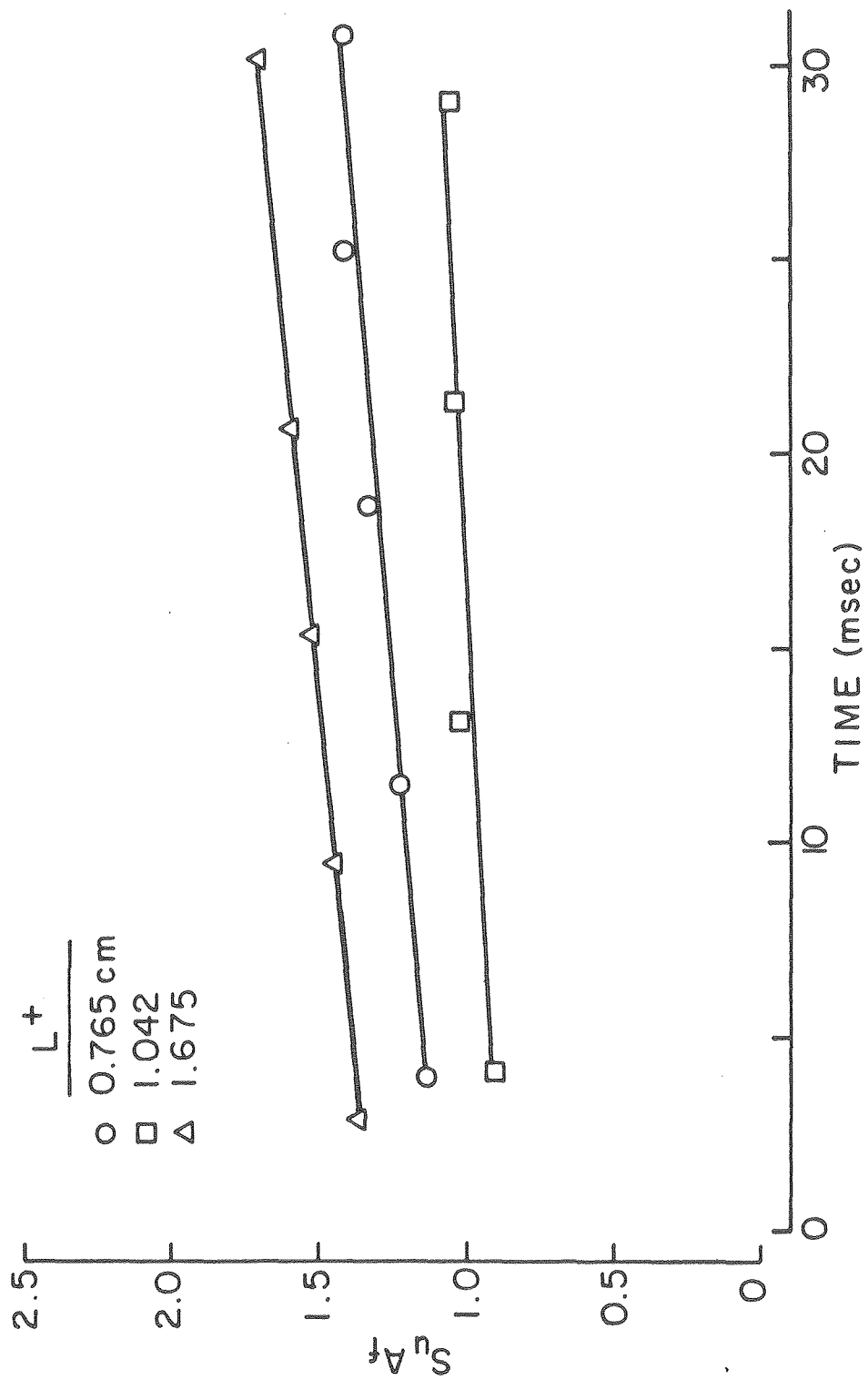
XBL 798-6777



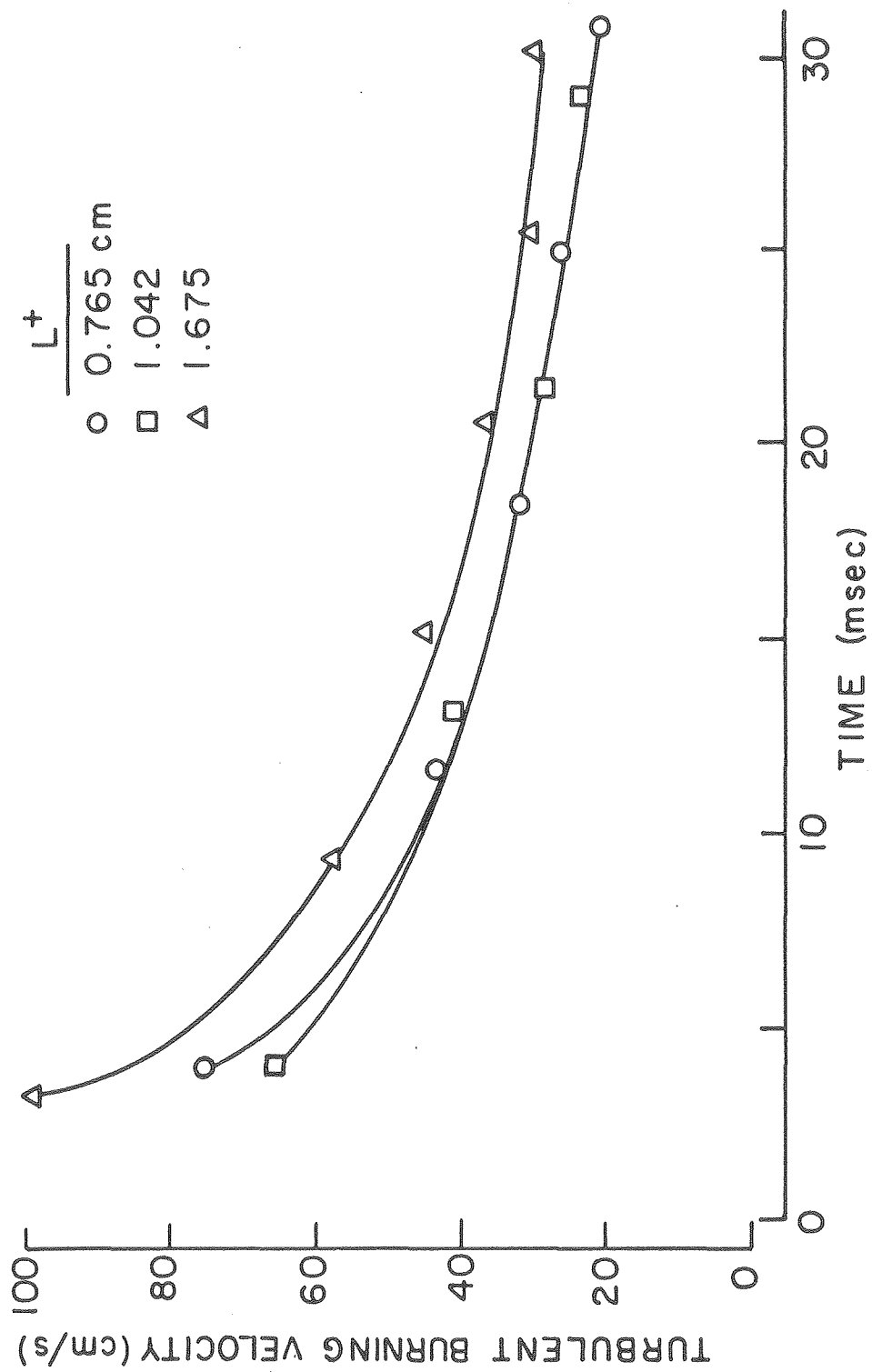
XBL 798-6778



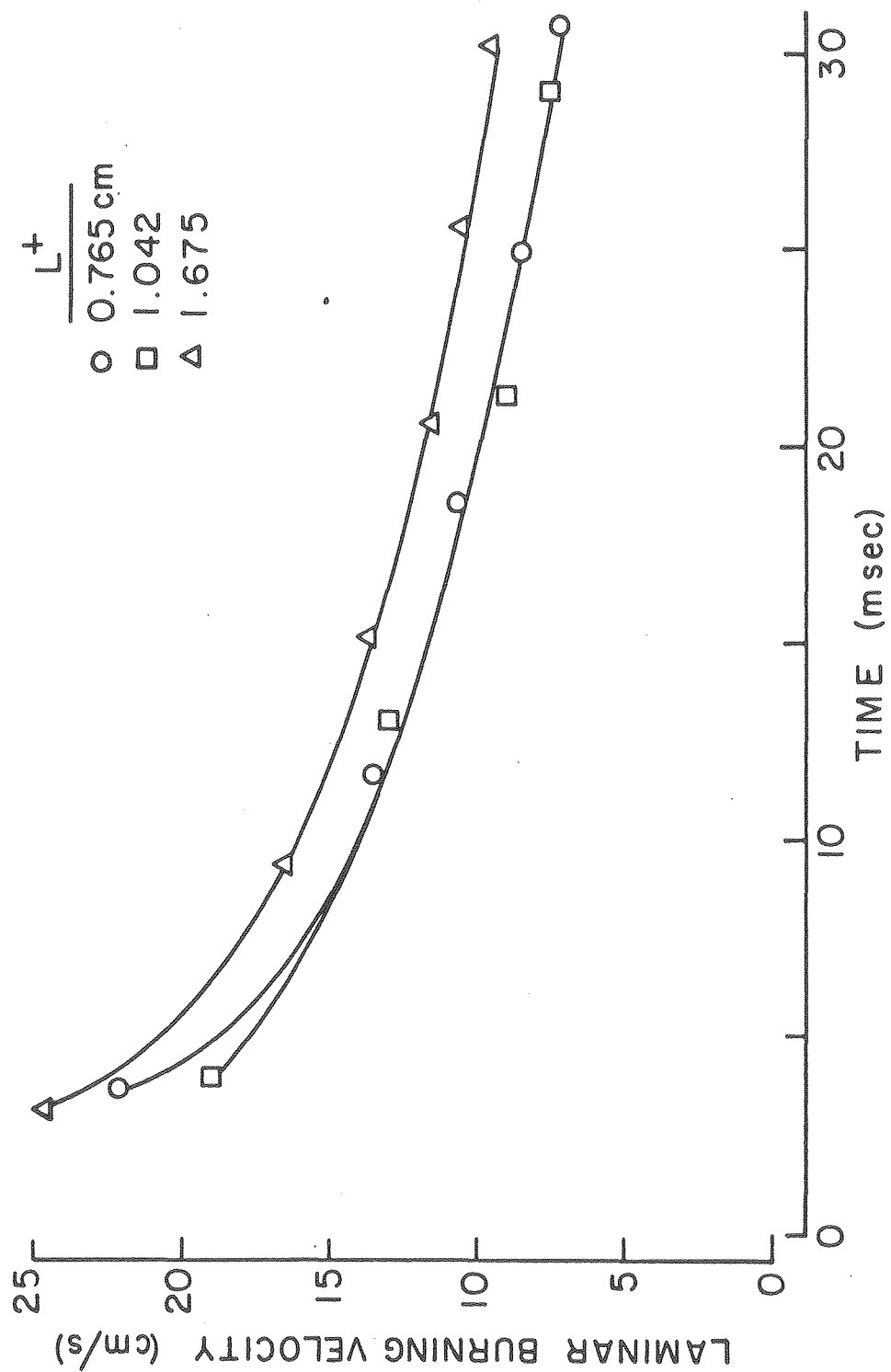
XBL 798-6779



XBL 798-6774

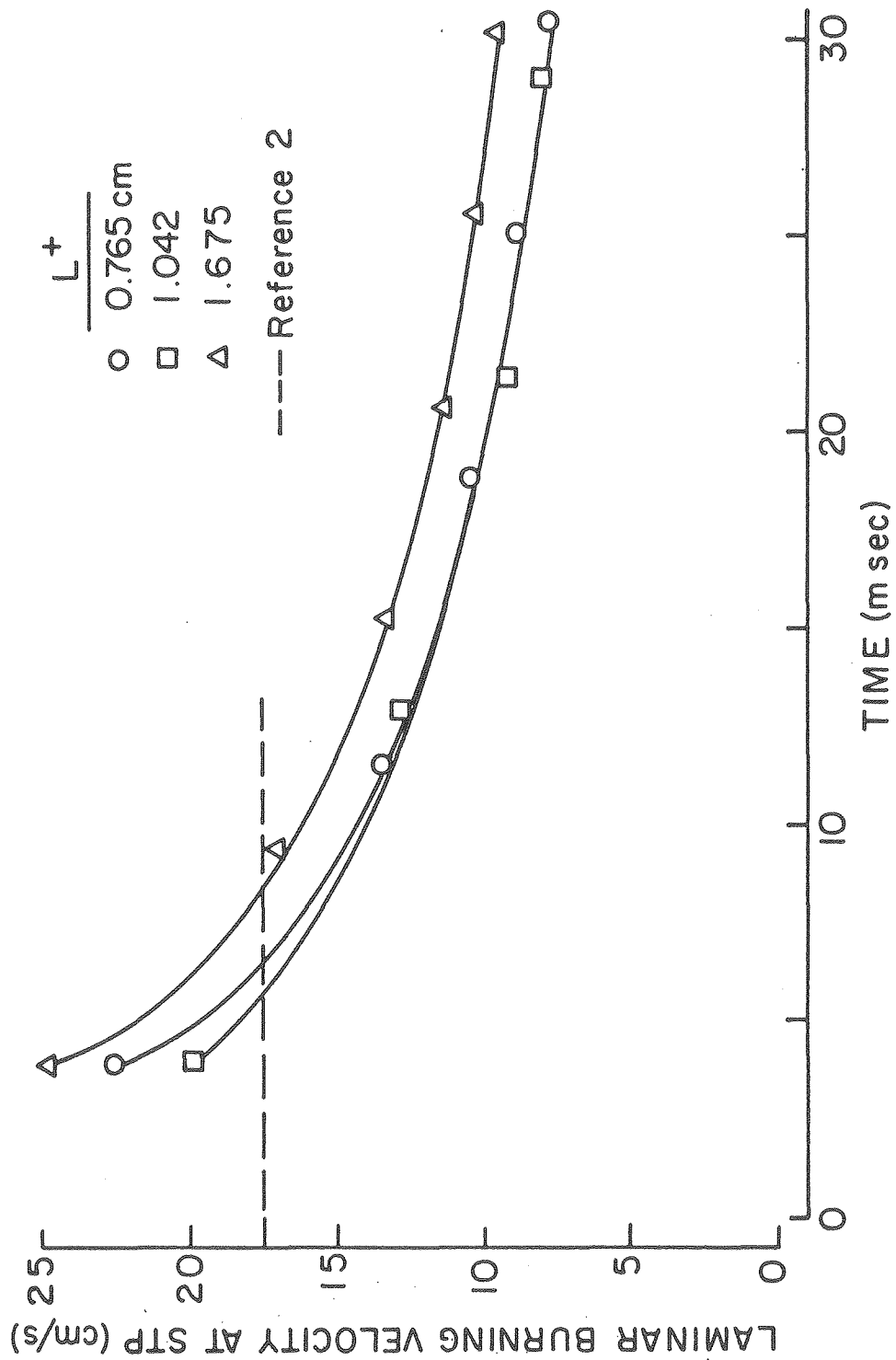


XBL 798-6780

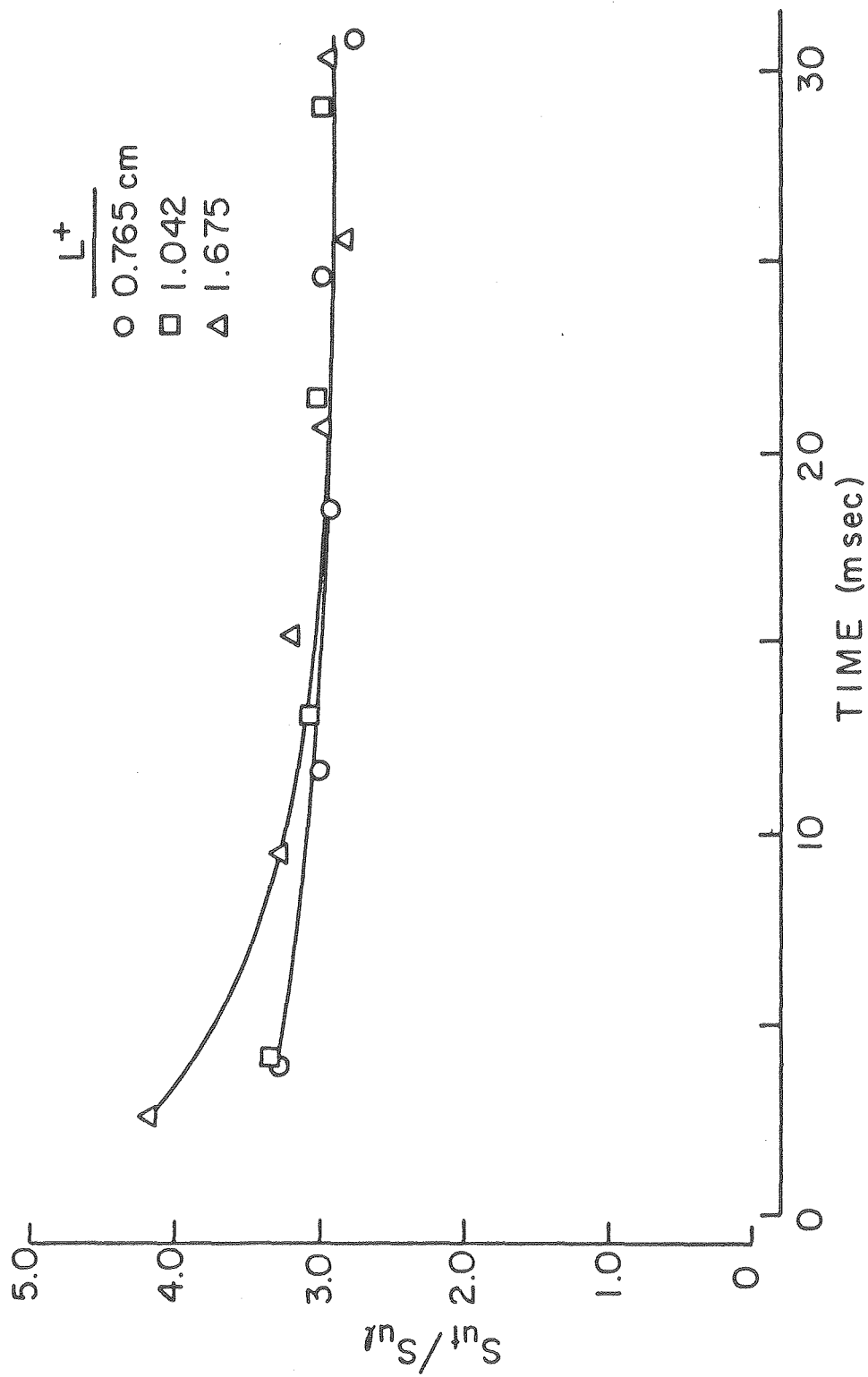


XBL798-6781

14



XBL798-6783



XBL 798-6773

